Frequency Response of PV Inverters Toward High Renewable Penetrated Distribution Networks

Feifei Bai, *Senior Member*, *IEEE*, Yi Cui, *Senior Member*, *IEEE*, Ruifeng Yan, *Member*, *IEEE*, Tapan Kumar Saha, *Fellow*, *IEEE*, Huajie Gu, and Daniel Eghbal, *Senior Member*, *IEEE*

***Abstract*—Substantial usage of electronic-based renewable energy resources has completely changed the dynamic behaviours and response time of power networks, which are now fundamentally different from traditional power networks dominated by Synchronous Generators (SGs). This paper evaluates the dynamic response of small-scale Photovoltaic (PV) inverters, which dominate the distribution networks and influence the dynamics of the entire power grid. Recently, some critical events which occurred in Australia have shown that the dynamic responses of small-scale inverters do not always follow the inverter standards. Subsequently, these uncertainties make PV inverters' response unpredictable and have the potential to threaten the security of power networks. The detailed investigation of the dynamic response characteristics of small-scale PV inverters to grid disturbances is lacking in the current literature. This paper presents new findings from experimental testing under extensive network disturbance scenarios. Furthermore, a data-driven method is proposed to accurately describe the dynamics of solar PV subjected to various frequency disturbances. The results provide beneficial insight to the network operators in predicting power system response to extreme disturbances and avoiding potential grid instability issues, which will assist in achieving 100% penetration of power electronics-based renewable energy resources in the future.**

***Index Terms*—Deep learning, distribution networks, dynamic response, distributed PV, load modelling, PV inverter.**

I. Introduction

OVER the last decade, the increase of electronic-based devices (e.g., wind and solar PV) has significantly changed the dynamic responses of traditional power systems dominated by SGs [1], [2]. Such a transition to a more power-electronized network has raised a concern to achieve safe operations of the system, including unanticipated cascading failures, low system inertia and unexpected need for real power reserves [3]. For example, right before the 2016 South Australia (SA) Blackout, PV and wind provided half of the total power generation of SA, while conventional SGs only accounted for 17.6% while other sources were provided by interconnections. The SA blackout occurred under the exact conditions of high renewable penetration with low inertia, which has brought new risks to grid control. To better manage the high renewable energy penetrated power grid, the key issue is to understand the dynamic response behaviors of the electronic-based devices. In particular, the dynamic response of PV inverters under frequency events has the most interest due to the reported catastrophic electricity outages as mentioned in the following section. Therefore, this paper will focus on realizing the dynamic frequency response of PV inverters and extracting associated characteristics through extensive laboratory experiments.

A. Solar PV Integration Background of Australia

Over the last ten years, Australia has witnessed an unprecedented increase in PV installation from about 163 MW in January 2010 to around 23.5 GW by September 2021 [4]. There are over 2.96 million PV installations in Australia and over 2 million residential PV installations expected until September 2021. As shown in Fig. 1, the total capacity of the residential solar PV is playing a dominant role in each state. Therefore, research about the dynamic response of small-scale inverters is crucial for the secure operations of the whole Australian power grid. However, given the large volume of small-scale PV inverters in the solar market, there is a lack of understanding of the dynamic behaviors of these PV inverters responding to the network frequency disturbances [5].

B. Australian Power Grid Events Relevant to Distributed Solar PV

Some recent events which occurred in Australia have shown that small-scale inverters do not always follow the Australian inverter standard AS 4777, which makes their dynamic behaviors difficult to predict. For example, during the 2018 Queensland and South Australia separation event (QLD-SA separation), an unexpected 450 MW reduction was observed in the distributed PV power generation [6]. Another recorded event shows that a 150 MW generation trip from a rooftop PV generation occurred in the 2017 Torrens Island Switchyard Fault [7]. The following analysis of the QLD-SA separation event provides more details of the unexpected response behaviors of distributed solar PV systems.

Manuscript received November 14, 2021; revised December 31, 2021, accepted January 25, 2022. Date of online publication February 14, 2022, date of current version February 16, 2022.

F. F. Bai, Y. Cui, R. F. Yan (corresponding author, e-mail: ruifeng@itee.uq.edu.au) and T. K. Saha are with the School of Information Technology and Electrical Engineering, the University of Queensland, Brisbane, QLD 4072, Australia.

F. F. Bai is also with the School of Engineering and Built Environment at Griffith University, Gold Coast, QLD 4222, Australia.

H. J. Gu is with the Australian Energy Market Operator (AEMO), Brisbane, QLD 4000, Australia.

D. Eghbal is with Energy Queensland (Energex), Brisbane, QLD 4006, Australia.

DOI: 10.17775/CSEEJPES.2021.08470

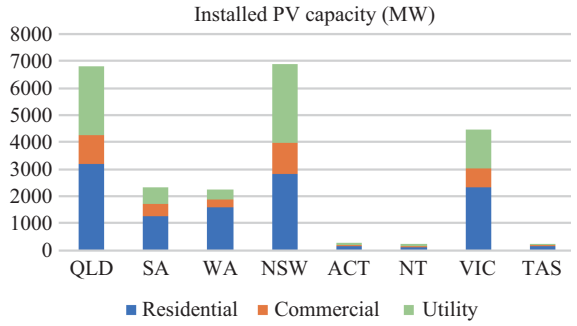

Fig. 1. Installed PV generation capacity of each state in Australia [4].

The Australian Energy Market Operator (AEMO) has reported that the QLD-SA separation incident [6] happened on August 25, 2018, where QLD was islanded and SA was separated from the National Energy Market (NEM). Such a separation further introduced 997.3 MW under-frequency load shedding of New South Wales (NSW), Victoria (VIC), and Tasmania (TAS). The recorded frequency response of each state is shown in Fig. 2.

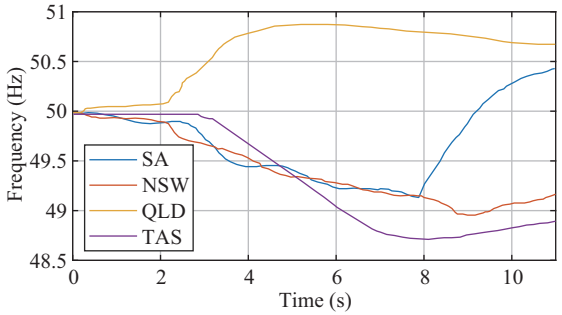

Fig. 2. Dynamic frequency response during the QLD-SA separation [6].

During this incident, there was a significant solar power generation drop induced by distributed PVs in QLD, SA, VIC and NSW. The reason for such tripping is still unclear and AEMO suspected that there was a high possibility that the response of distributed PV inverters to frequency events may not be compliant with the relevant Australian standard. Specifically, the PV systems installed before Oct 2015 should follow the AS4777.3-2005 (old standard) [8], and the PV systems commissioned after Oct 2016 should follow the AS/NZS 4777.2-2015 (new standard) [9], while the PV systems installed in between can choose either one. The frequency requirement in both standards is shown in Fig. 3. The PV inverters following the old standard should not disconnect under frequency disturbances between 45 Hz and 55 Hz. For the PV inverters following the new standard, they should not disconnect or change power output under frequency disturbances between 49.75 Hz and 50.25 Hz. For disturbances from 50.25 Hz to 52 Hz, the PV power output should be linearly reduced to provide necessary frequency support to the network.

However, further investigations from AEMO (shown in Table I) revealed that not all the PV inverters complied with these two standards during the QLD-SA Separation [6]. Taking

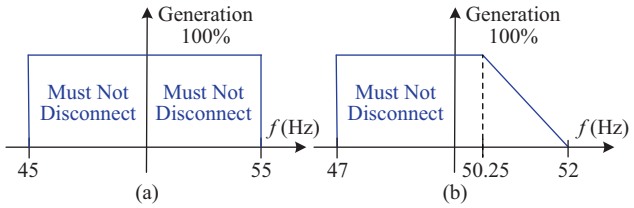

Fig. 3. Response of PV inverters to frequency variations required by (a) AS 4777.3-2005 (old standard) and (b) AS/NZS 4777.2-2015 (new standard).

TABLE I
DISTRIBUTED PV INVERTER RESPONSE TO FREQUENCY CHANGE [6]

Compliance of PV systems	Region	Percentage of the PV inverter response to the frequency change
AS 4777.3-2005	QLD	∼15% of the PV inverters' frequency response does not follow the standard and should not be disconnected
	SA	∼13% of the PV inverters' frequency response does not follow the standard and should not be disconnected
AS/NZS 4777.2-2015	QLD	At least 15% of inverters did not exhibit the over-frequency reduction
	SA	At least 30% of inverters did not exhibit the over-frequency response
	VIC	∼8% of the PV inverters' frequency response does not follow the standard and should not be disconnected
	NSW ACT	∼10% of the PV inverters' frequency response does not follow the standard and should not be disconnected

the PV inverters of QLD as an example, 15% of the PV inverters regulated by the old standard should have remained connected. What was even more unexpected is that at least 15% of the PV inverters following the new standard did not exhibit the required frequency response. These unexpected behaviors of PV inverters have significantly influenced the system frequency dynamics and they may further lead to grid instability issues (e.g., cascading frequency drop) when substantial PV inverters are disconnected.

The distributed PV inverter response in this event is a typical example of worldwide high solar PV integrated networks. The unpredictable solar PV system connections and the unknown solar PV inverter responses make the power reserve estimation more difficult and the dynamics of the whole power grid become invisible under disturbances. Therefore, power networks are becoming more vulnerable to disturbances, which may cause more unacceptable and widespread impacts.

C. Research Gaps and Contributions

The largely unknown behaviors of PV inverters have raised an urgent need for the accurate estimation of the dynamic response of distributed PV inverters. The existing distributed generator model [10] used by power industries is a piece-wise linear function of bus voltage and the frequency impact is not considered in this model. This model is over-simplified and no longer suitable to represent the actual dynamics of the PV inverter. Therefore, the network operators have the desire to understand the dynamic response behaviors of the small-scale inverters and develop new models of the dynamic behavior of electronic-based load.

1) Dynamic frequency response behavior testing of distributed PV inverters

The existing experimental testing of PV inverter dynamic response is primarily focusing on the utility-scale PV inverters [11], [12]. The dynamic response of small-scale PVs (e.g., 5 kW) integrated at the rooftop is often overlooked as these PV systems are often thought to be too small to impact the bulk power grid compared with the large-scale PV systems. This assumption is true for a single PV inverter. However, the combined impact of all the small-scale PV systems will become significant to the entire power system. The active power responses of residential PV inverters are usually tested by the manufacturers through a series of step disturbances of bus voltage and frequency. But the step disturbances cannot fully reflect the network disturbances. For example, the QLD-SA separation event also evidenced that not all the inverters were compliant with the inverter standard. Moreover, the frequency support provided by the small-scale PV inverters has been neglected as most testings focus on the voltage sags and swells [13], [14]. In addition, the unknown response behaviors of small-scale inverters also create significant challenges to the feeder-level load modeling since the PV inverters are complex power electronic-based devices and their detailed model information is not publicly available due to the confidentiality of commercial Intellectual Property (IP) of PV manufacturers. Therefore, this paper focuses on the testing of the frequency response characteristics of residential PV inverters from two manufacturers who hold the dominant share in the Australian solar market.

2) Bottom-up estimation of individual small-scale PV dynamic response behaviors

Transmission-level and distribution feeder-level response estimation of aggregated PV systems have been investigated in numerous literature [15]–[17]. Most of the current residential load dynamic response estimation focuses on characterizing the total power consumption profiles of residential load and PVs under steady-state conditions [18], [19]. It is lacking the estimation of the dynamic response behaviors of individual residential PV inverters subjected to different network disturbances. However, the feeder-level PV inverter dynamic response estimation can be inaccurate if it is unaware of the individual dynamic response behaviors of the PV inverters. Therefore, this paper conducts the bottom-up modeling of the dynamic response from different individual PV inverters based on the extracted dynamic response characteristics through experiments.

The dynamic response estimation methods can be divided into two categories: component-based [21], [22] and data-driven approaches [24]–[26]. The component-based approach requires prior knowledge of the physical characteristics and mathematical relationships that describe the functionality of the PV inverters. For instance, the distributed PV system model (PVD1) [23] developed by the WECC working group includes detailed mathematical inner control loops of PV inverters. The PVD1 model can represent the voltage and frequency response of PV inverters with reasonable accuracy if the parameters can be appropriately identified. However, this model is very difficult to be implemented to estimate the actual PV inverter response. On the one hand, it is very hard to determine the proper model parameters of PVD1 due to too many control logics and parameters in this model [13], [28]. On the other hand, the lack of details and the emerged new technologies of PV inverters can further hinder the component-based approaches. With data acquisition technology development, data-driven approaches become popular. Since the PV inverter dynamic response refers to the mathematical relationship representation of the inputs (network frequency and voltage) and outputs (active power and reactive power) of the PV system, the equivalent response of PV inverters can be simplified with the input-output relationships. Based on the response of PV systems to disturbances (e.g., voltage disturbances and frequency disturbances), the PV dynamic model can be formed with voltage/frequency-dependent and independent components. For example, the US Electric Power Research Institute (EPRI) developed the EPRI LOADSYN model [29] and this mathematical model with physical meaning has been widely used for estimating the dynamic behaviors of both individual load (a specific device) and aggregated load (whole feeder), which combines ZIP, exponential, and frequency-dependent models. However, the responses of inverters may not be able to be modeled by equations with physical meanings due to the complexity of electronic components. Artificial intelligent technologies are often utilized to model complex response behaviors by mapping the input data set to the output dataset through the training and testing process [30], [31]. The advantage of this type of data-driven approach is that there is no need for prior knowledge of the inner control loops of inverters and it can be adapted to different operating conditions with online model updating. In this paper, the data-driven approach is used to estimate the dynamic response behaviors of individual small-scale PV inverters.

This paper intends to extract the dynamic frequency response characteristics of different residential inverters and build models to estimate their dynamic responses. The main contributions of this paper are:

- An innovative controllable hardware testbed is established based on the Real-time Digital Simulator (RTDS) for the small-scale solar PV inverter testing.
- New frequency response characteristics are revealed and extracted from different inverters through extensive laboratory experiments.
- A data-driven frequency response estimation approach is proposed to estimate the active power output of PV inverters under various frequency disturbances. The effectiveness of the proposed approach has been demonstrated through a comparative study with the existing approach.

The experimental results and the proposed approach have the potential to assist the network operators in determining the root causes of unexpected PV inverter responses to network events. Moreover, the extracted behaviors and the developed inverter frequency response estimation approach can benefit the top-down estimation of dynamic response from the aggregated PV systems at both the feeder level and transmission level.

II. Dynamic Characteristics Extraction from Frequency Response

A. Established Testbed

An experimental testbed is built to test the dynamic response of PV inverters as illustrated in Fig. 4. The reporting rate of RTDS is within the range of 5–10 μs, which is high enough to capture the dynamics during the imposed disturbances. First, a wide range of frequency events are simulated in RTDS. Then the simulated events are transferred through an analog output card (GTAO) with small magnitude to power amplifiers, by which the signals are boosted from 2.3 V to 230 V to form a controllable grid. In this way, the original frequency signals are able to replicate the events that occurred in a real-life network. After the amplified events are applied to the PV inverters, the corresponding responses are measured and sent back to RTDS through an analog input card (GTAI). All measured signals are automatically synchronized within RTDS. At the same time, the power, frequency and voltage are recorded by a Phasor Measurement Unit (PMU) with a sampling rate of 100 Hz. Overall, the experimental setup in Fig. 4 can provide a controllable, complete and repeatable platform for testing the dynamic responses of various small-scale PV inverters under different frequency events.

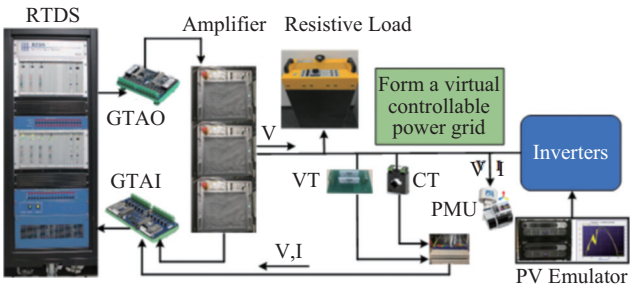

Fig. 4. Developed inverter testing platform.

B. Experiment Scenarios

In order to show the major dynamic responses of small-scale PV inverters, four widely used PV inverters manufactured by the two most popular manufacturers (denoted as Inv-A and Inv-B in Table II) in the Australian solar market are selected. Two inverters complying with AS4777.3-2005 (old standard) and AS/NZS 4777.2-2015 (new standard) (denoted as new and old in the bracket in Table II) are selected from each manufacturer. This will help to achieve a direct comparison of the dynamic response of each type of PV inverter. The detailed testing scenarios for each inverter are shown in Table II. A total of 25 under-frequency disturbances are generated when the frequency nadir changes from 47 Hz to 49.4 Hz with a step of 0.1 Hz. The schematic shape of the frequency disturbance curves is shown in Table II. It should be noted that the over-frequency scenarios are not considered since the over-frequency events are relatively easier to manage as excessive power can be cut to maintain the grid frequency.

TABLE II
Experiment Scenarios for Inverters

Cases	Frequency disturbance	Inverters
Under frequency events (25 cases)	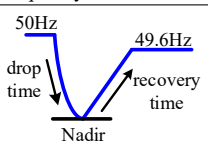	Inv-A (old), Inv-A(new), Inv-B (old), Inv-B (new): Single-phase Voltage: 230 V Power: 5 kW

C. Dynamic Response Characteristics During Disturbances

The summary of the dynamic responses of each inverter after 25 frequency disturbances are presented in Table III. It can be found that only Inv-A(old) and Inv-B (new) can successfully ride through the frequency disturbances as required by the standard. Inv-A(old) can ride through the frequency events when the frequency nadir is higher than 47.4 Hz. But the Inv-B (old) is very sensitive to the frequency variations as it finally returns to its normal state after several temporary disconnections. The typical frequency response details of each inverter corresponding to three frequency disturbance scenarios (47.2 Hz, 48.5 Hz, and 48.9 Hz) are shown in Fig. 5.

TABLE III
Experiment Results

Inverters	Inverter responses under frequency events
Inv-A(old)	• No disconnection in 25 cases (47 Hz $\leq f_{\text{nadir}} \leq$ 49.4 Hz) • Provide frequency support
Inv-A(new)	• Disconnected when $f_{\text{nadir}} \leq$ 47.4 Hz • Provide frequency support
Inv-B(old)	• Disconnected when $f_{\text{nadir}} \leq$ 47.2 Hz • Reboot when 47.3 Hz $\leq f \leq$ 48.5 Hz • No frequency support
Inv-B(new)	• No disconnection in 25 cases (47 Hz $\leq f_{\text{nadir}} \leq$ 49.4 Hz) • No frequency support

As shown in Fig. 5(b), the Inv-A (new) and Inv-B (old) are disconnected before the frequency dropped to the lowest connection frequency 47 Hz. Inv-A (old) and Inv-B (new) to maintain the connection during the frequency event but they have different response behaviors. The power output of the Inv-A (old) will increase and decrease with frequency drop and recovery, respectively. In comparison, the power output of the Inv-B (new) is almost constant with very slight power variations.

From Fig. 5(c) it is clear that all the inverters can successfully ride through the frequency disturbances except Inv-B (old). The Inv-B (old) disconnects twice from the grid and reboots the connection within one second. In terms of Fig. 5(d), all the inverters are keeping the connection with the power grid during the under-frequency events but have different dynamic response behaviors. The power output of the Inv-B (new) is close to constant. By contrast, the dynamic response of Inv-A (old) and Inv-A (new) can support the network frequency with power increases during the under-frequency event while the Inv-B (old) will aggravate the under-frequency problems with power decreasing under the frequency drop events.

In summary, Inv-A (old) can provide frequency support during under-frequency events while Inv-B (old) is very sensitive

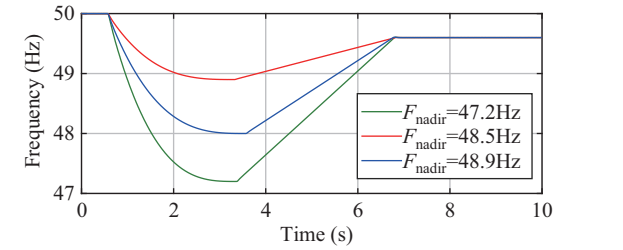

(a) Typical examples of frequency disturbances in three scenarios

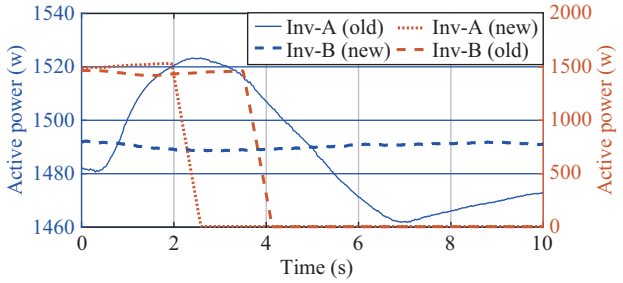

(b) Typical frequency response of Scenario 1 (frequency nadir is 47.2Hz)

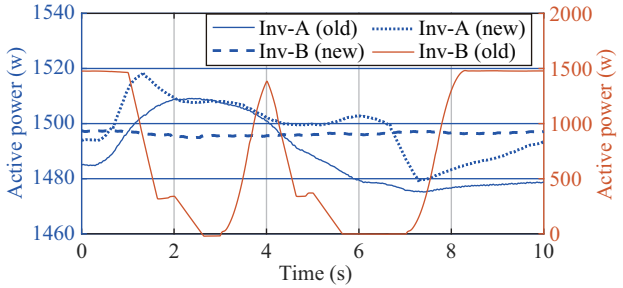

(c) Typical frequency response of Scenario 2 (frequency nadir is 48.5Hz)

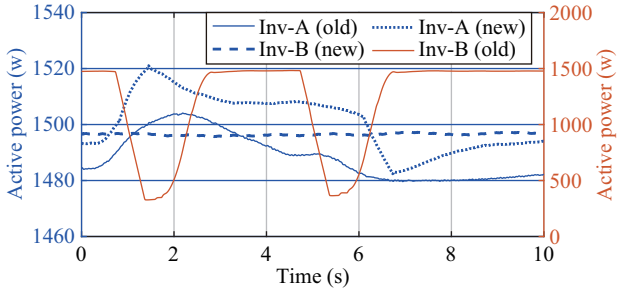

(d) Typical frequency response of Scenario 3 (frequency nadir is 48.9Hz)

Fig. 5. PV inverter dynamic responses under different frequency events.

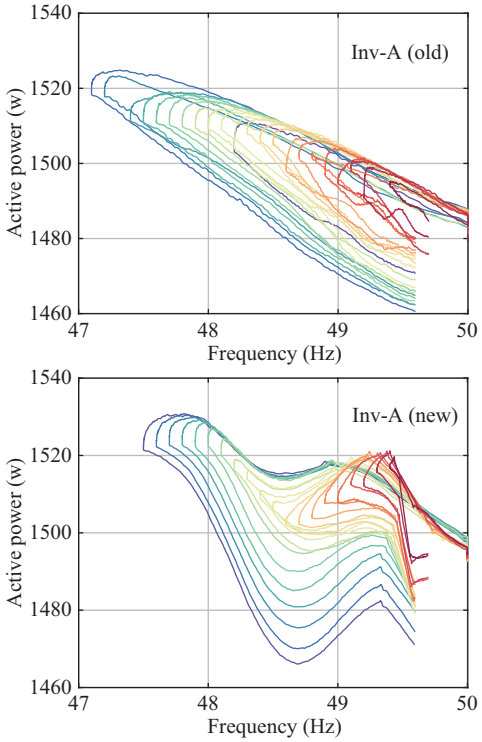

Fig. 6. Characteristics of frequency variations and the active power of Inv-A.

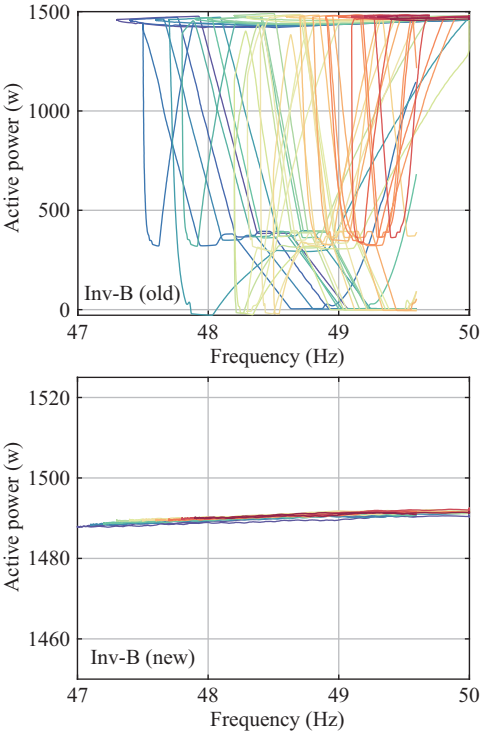

Fig. 7. Characteristics of frequency variations and the active power of Inv-B.

to frequency variations and against frequency recovery. Inv-A (new) also can provide frequency support when the frequency nadir is above 47.4 Hz. Inv-B (new) is compliant with the new Standard during under-frequency events. In addition, Inv-A (new) and Inv-B (old) can be disconnected from the grid before the frequency drops to the lowest connection frequency of 47 Hz.

D. Inverter Response Characteristics

In order to explore the frequency response features of different inverters, the characteristics of PV power output changes of Inv-A and Inv-B are extracted as shown in Fig. 6 and Fig. 7, respectively. The different colors of curves in these two figures represent different power output under 25 disturbance scenarios. For Inv-A, the power output shows a high dependency on the frequency. It increases when the frequency drops. In other words, the inverters from manufacture A have frequency support during the frequency disturbances. However, the variation trends of the power output from Inv-A (old) and Inv-A (new) are different. An approximately linear

relationship is presented between the power output of Inv-A (old) and the network frequency while for Inv-A (new), such a relationship is more complex.

Figure 7 shows the power output of Inv-B during different frequency disturbances. Significant differences are observed from the measured frequency response of two types of inverters. Compared with Inv-B (old), the power output of Inv-B (new) has a minimal change which demonstrates that Inv-B (new) is less dependent on the frequency. For Inv-B (old), there is no clear pattern between the frequency variations and the active power output. Moreover, Inv-B (old) can be either disconnected or connected to the power network with the same frequency. Therefore, it is difficult to model the dynamic frequency response of Inv-B (old) through the simplified WECC DG models [10] and the EPRI LOADSYN.

The previous analysis demonstrates that each type of inverters has a unique dynamic response to frequency disturbances and it is hard to utilize a universal model with a physical meaning to fully describe the dynamic responses of different types of inverters. Therefore, a machine learning-based model is proposed in Section IV to provide a reasonable estimation of the active power change of the inverter when it is subjected to different frequency disturbances.

III. Data-driven Dynamic Frequency Response Estimation

A. Framework of Data-driven Frequency Response Estimation

The proposed data-driven response estimation framework is shown in Fig. 8, which primarily contains four steps: (1) collect the training and testing input data for feature extraction; (2) extract features for training and testing; (3) train the Multivariate Random Forest Regression (MRFR) algorithm [32] to build a mathematical model, which is representative of the extracted signatures and active power change; (4) implement the obtained MRFR model to estimate the active power change of the inverter by using the frequency measurements of the new disturbances. The output of the estimation is the active power of the PV inverters. It should be noted that some other machine learning algorithms can be used for frequency response estimation. However, MRFR is selected in this paper for good reasons. For example, it is easily implemented since it has fewer parameters that need to be tuned during the training process. In addition, it has high robustness to the input features which has the potential to avoid the over-fitting problem.

B. Feature Extraction for Frequency Response Estimation

The frequency response of PV inverters is primarily determined by the control strategies and associated parameters which are designed by the manufacturer. However, such detailed information is always inaccessible which cannot be used as the input features for frequency response estimation. Therefore, this paper uses two types of measurements, i.e., frequency data and active power of the inverter before the disturbance to extract the informative features for frequency response estimation.

1) Feature extraction from frequency measurement

To estimate the active power change of the inverter, data pre-processing, including data continuity check, outlier detection, and deletion, are performed on the original time series frequency data measured during the disturbance. Then the measured frequency data at each time instance during the disturbance as well as the Rate of Change of Frequency (ROCOF) in (1) are used as the informative signatures for active power change estimation.

$$\text{ROCOF}(t_i) = \frac{\mathrm{d}f}{\mathrm{d}t} = \frac{f(t_{i+1}) - f(t_i)}{t_{i+1} - t_i} \tag{1}$$

where $f(t_i)$ denotes frequency at i-th time instance t_i.

2) Feature extraction from the active power measurement

Besides frequency data, the steady-state active power of the inverter is also measured and it is used as input features for MRFR to estimate the subsequent active power change.

As can be seen from Fig. 9, the active power change of the inverter can be divided into two stages, i.e., Stage 1-response during frequency disturbance and Stage 2-post-disturbance response. The first stage of the active power change is dependent on the imposed frequency disturbance

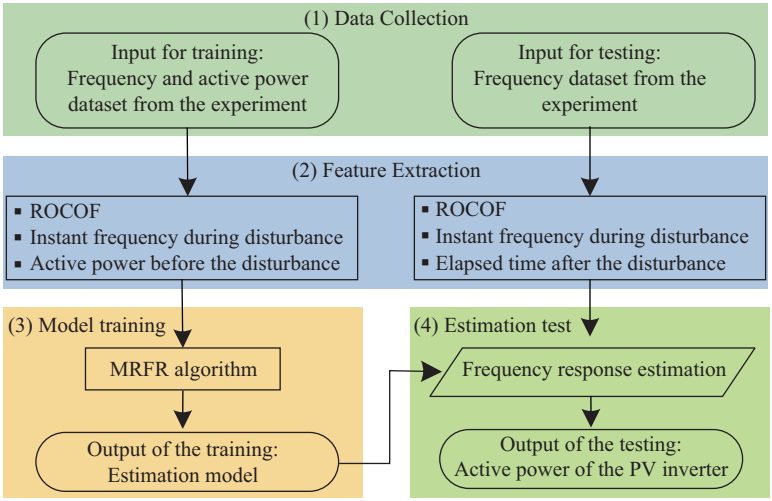

Fig. 8. Framework of the proposed data-driven frequency response estimation.

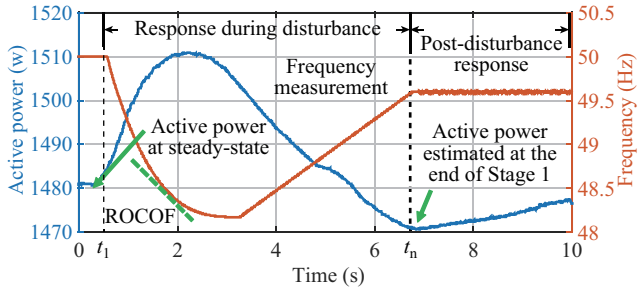

Fig. 9. Example of active power change during frequency disturbance and post-disturbance response and corresponding features for MRFR algorithms.

while the second stage of the active power change is primarily determined by the internal control strategy of the inverter since the imposed frequency is kept constant during this stage. Therefore, these two stages of the active power change are modeled sequentially using two MRFR models (i.e., MRFR1 and MRFR2). The major difference in estimating the response during frequency disturbance and post-disturbance lies in the input features of the MRFR which are shown in Table IV. The response during the disturbance primarily relies on the measured frequency while the post-disturbance response is primarily dependent on estimated active power at the end of Stage 1 and the elapsed time after the disturbance.

TABLE IV
FEATURE DECOMPOSITION OF RESPONSE ESTIMATION

Response during disturbance (modelled by MRFR1)	Post-disturbance response (modelled by MRFR2)
Frequency measurement $f(t_i)$ at each time instance t_i during the disturbance	Active power $P(t_1)$ measured at the steady-state t_1
ROCOF(t_i) calculated at each time instance t_i during the disturbance	Active power $P'(t_n)$ estimated by MRFR1 at the end of Stage 1 t_n
Active power $P(t_1)$ measured at steady-state t_1	Elapsed time after the disturbance $t_i - t_n, (n < i \leq m)$

For each frequency disturbance, a 10-second dynamic response (1,000 samples) of the inverter with a sampling period of 10 ms is collected. The collected frequency response is then formulated into two feature matrices for estimating the two parts (i.e., during disturbance and post-disturbance) of active power change as (2) and (3).

$$I_1 = \begin{bmatrix} f(t_1) & \text{ROCOF}(t_1) & P(t_1) \\ f(t_2) & \text{ROCOF}(t_2) & P(t_1) \\ \vdots & \vdots & \vdots \\ f(t_n) & \text{ROCOF}(t_n) & P(t_1) \end{bmatrix}, U_1 = \begin{bmatrix} P(t_1) \\ P(t_2) \\ \vdots \\ P(t_n) \end{bmatrix} \quad (2)$$

$$I_2 = \begin{bmatrix} P(t_1) & P'(t_n) & t_{n+1} - t_n \\ P(t_1) & P'(t_n) & t_{n+2} - t_n \\ \vdots & \vdots & \vdots \\ P(t_1) & P'(t_n) & t_m - t_n \end{bmatrix}, U_2 = \begin{bmatrix} P(t_{n+1}) \\ P(t_{n+2}) \\ \vdots \\ P(t_m) \end{bmatrix} \quad (3)$$

where I_1 and I_2 denote the feature matrices of active power change during and after the frequency disturbance, U_1 and U_2 are the corresponding estimation target, t_n is the last time instance of the response during the disturbance, $t_m = 10$ s is the total time of each collected response, P and P' are measured and estimated active power.

C. Multivariate Random Forest Regression

The feature matrix extracted from frequency responses under multiple disturbances is collected to establish a data pool for training the MRFR so that the algorithm can establish a mathematical relationship between the extracted features and the estimation target. As shown in Fig. 10, for MRFR, it first uses bootstrap to select S samples in the training data pool. Then, a subset of the features (i.e., D-dimension) of each selected sample is picked up. Afterwards, the parent node of a decision tree $\varnothing$ is divided into two children nodes based on the impurity function of the subset features [32]. Each terminal node of the decision tree went through the same process until the minimum node size reaches the predefined value. The well-trained decision tree is further utilized to provide an estimation of the frequency response by using the feature matrix of frequency response under the new disturbance. The above procedure is iterated for k times and the estimation results during each iteration are averaged out to provide the final frequency response estimation of the new disturbance.

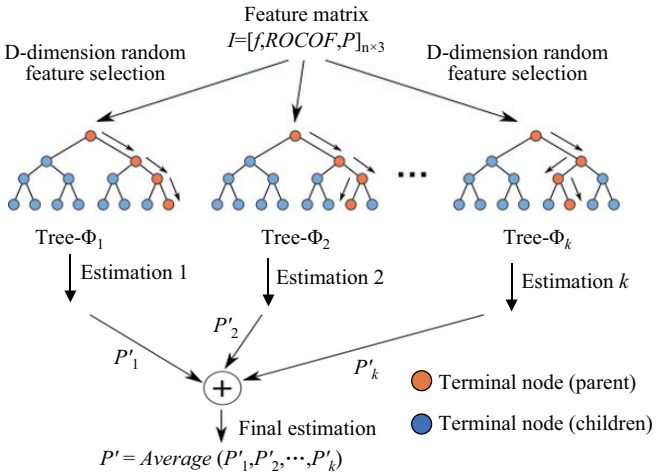

Fig. 10. Schematic diagram of frequency response estimation using MRFR.

IV. CASE STUDY AND METHODOLOGY VERIFICATION

A. Testing Setup and Evaluation Metrics

The proposed data-driven dynamic frequency response estimation framework is implemented to estimate the active power change of four types of inverters with each being subjected to 25 frequency disturbances. It primarily contains three steps: (1) Informative features relevant to PV inverter's frequency response are extracted from the frequency data and active power measurements in the training dataset; (2) The extracted features are used to train the MRFR to model the potential relationship between the extracted features and the active power of PV inverters; (3) The above trained MRFR model is further implemented to estimate the active power of PV inverters by using the features extracted from the frequency data and active power measurements in the testing dataset. For each type of inverter, active power change under one frequency disturbance is selected as the estimation target while the active power during the rest of the disturbances is used for training the MRFR. During the training process, multifold

cross-validation is performed to determine the optimal values of the parameters of the MRFR, including the total tree number of the forest (i.e., 500), minimal leaves of each regression tree (i.e., 50) and number of features that are randomly selected by each tree (i.e., 3). Some software routines in [32] are tailored for the algorithmic implementation in this study. Coefficient of determination (R^2) between the measured and estimated active power change is selected as a performance evaluation metric, which is shown in (4). The normal range of R^2 is between [0, 1] where $R^2 = 1$ means the estimation model has full capability to describe the active power change.

$$R^2 = 1 - \frac{\sum_{i=1}^{N} (P_i' - P_i)^2}{\sum_{i=1}^{N} (P_i - \overline{P})^2} \tag{4}$$

where N denotes the sample size of the measured active power change for each frequency disturbance, P_i' and P_i denote the i-th sample of the estimated and measured active power, $\overline{P}$ denotes the mean value of the measured active power.

All experiments are performed using a general desktop with an Intel Core i7-10700 CPU and 32 GB RAM. For each type of PV inverter, it takes about 10 seconds for the MRFR training. After training, the active power of the PV inverter at a single time instance can be estimated using the trained model within 5 ms. Given the reporting rate of the PMU used in the experiment is 10 ms per sample, the proposed method can provide online frequency response estimations of PV inverters using high reporting rate PMU measurements.

B. Estimation Results Analysis

Based on the frequency response behaviors extracted in Section II-D, some inverters have frequency-dependency characteristics and some inverters have constant power during frequency disturbances. To demonstrate the superiority of the proposed method, the EPRI LOADSYN model [29] was selected in the comparative study due to its wide usage for estimating the dynamic behaviors of both individual load and aggregated load. The EPRI LOADSYN model combines ZIP, exponential, and frequency-dependent models as shown in (5). It should be noted that the output voltage of the power amplifiers is kept as a constant at 1pu during the frequency disturbance. Therefore, the active power of the EPRI model is primarily dominated by the frequency-dependent component.

$$P = P_0 \left[P_a \left(\frac{V}{V_0} \right)^{K_{v1}} \left(1 + K_f \cdot \frac{f - f_0}{f_0} \right) + (1 - P_a) \left(\frac{V}{V_0} \right)^{K_{v2}} \right] \tag{5}$$

where P_0 is the active power of the inverter at the rated voltage V_0 and nominal frequency f_0, P_a is the fraction of the active power which is dependent on the frequency, K_f is the sensitivity coefficient of active power, K_{v1} and K_{v2} are voltage exponents for frequency-dependent and independent active power. The values of parameters P_a, K_f, K_{v1} and K_{v2} are determined through the least square method for each frequency disturbance.

The frequency response estimation results of four inverters under disturbances with the nadirs of 48 Hz and 48.5 Hz are shown in Fig. 11. Table V compares the R^2 of the active power response estimated by the proposed method and EPRI model under two frequency disturbances (48 Hz and 48.5 Hz nadir) as well as the overall R^2 of frequency response over 25 disturbances. The R^2 values are calculated over the whole frequency disturbance period, which is 10 seconds in Fig. 11.

As presented in Fig. 11 and Table V, for Inv-A (old), Inv-A (new) and Inv-B(new), the proposed method can provide an accurate estimation of the dynamic frequency responses with an overall R^2 greater than 0.9. The response estimation accuracy of Inv-B (old) is a little bit lower (overall R^2 of 0.85) than that of other inverters. However, the developed estimation model can still capture the major variation trend of the Inv-B power output while the EPRI model is unable to provide a reliable estimation. The response estimation error of the Inv-B (old) is due to the complexity of its frequency response characteristics as shown in Fig. 7. Compared with the estimation results of the EPRI model, the proposed method shows significantly higher accuracy in the estimated dynamic frequency responses of Inv-A (old), Inv-A (new) and Inv-B(old). For Inv-B (new), the proposed method and the EPRI model produce comparable results with a R^2 of 0.8 since the active power response of Inv-B (new) is less dependent on the frequency disturbance.

TABLE V
COEFFICIENT OF DETERMINATION (R^2) OF ACTIVE POWER RESPONSE ESTIMATED BY THE PROPOSED METHOD AND EPRI MODEL

Inverters	Proposed method			EPRI model		
	48 Hz	48.5 Hz	Overall	48 Hz	48.5 Hz	Overall
Inv-A(old)	0.99	0.98	0.92	0.44	0.33	0.46
Inv-A(new)	0.99	0.96	0.96	0.42	0.32	0.38
Inv-B(old)	0.97	0.78	0.85	0	0	0.04
Inv-B(new)	0.7	0.7	0.8	0.7	0.7	0.8

To demonstrate the advantages of the MRFR algorithm in estimating the frequency response of PV inverters, Table VI compares the overall R^2 of active power response estimated by other machine learning methods, including the k nearest neighbor with uniform weights - kNN_Uni, k nearest neighbor with inversely proportional distance weights – kNN_Dis and decision tree regressor - DT. It shows the estimation accuracy of these three machine learning algorithms is lower than the MRFR. However, they all outperform the EPRI model in estimating the frequency response.

TABLE VI
OVERALL COEFFICIENT OF DETERMINATION (R^2) OF ACTIVE POWER RESPONSE ESTIMATED BY OTHER MACHINE LEARNING METHODS

Inverters	KNN_uni	KNN_Dis	DT
Inv-A(old)	0.84	0.86	0.89
Inv-A(new)	0.77	0.77	0.92
Inv-B(old)	0.75	0.76	0.8
Inv-B(new)	0.8	0.8	0.8

C. Discussion for Future Study

This section discusses the potential of the proposed frequency estimation approach and future study for feeder-level frequency dynamic response estimation.

The barrier to the dynamic response estimation of small-scale PV inverters is the high diversity of dynamic responses

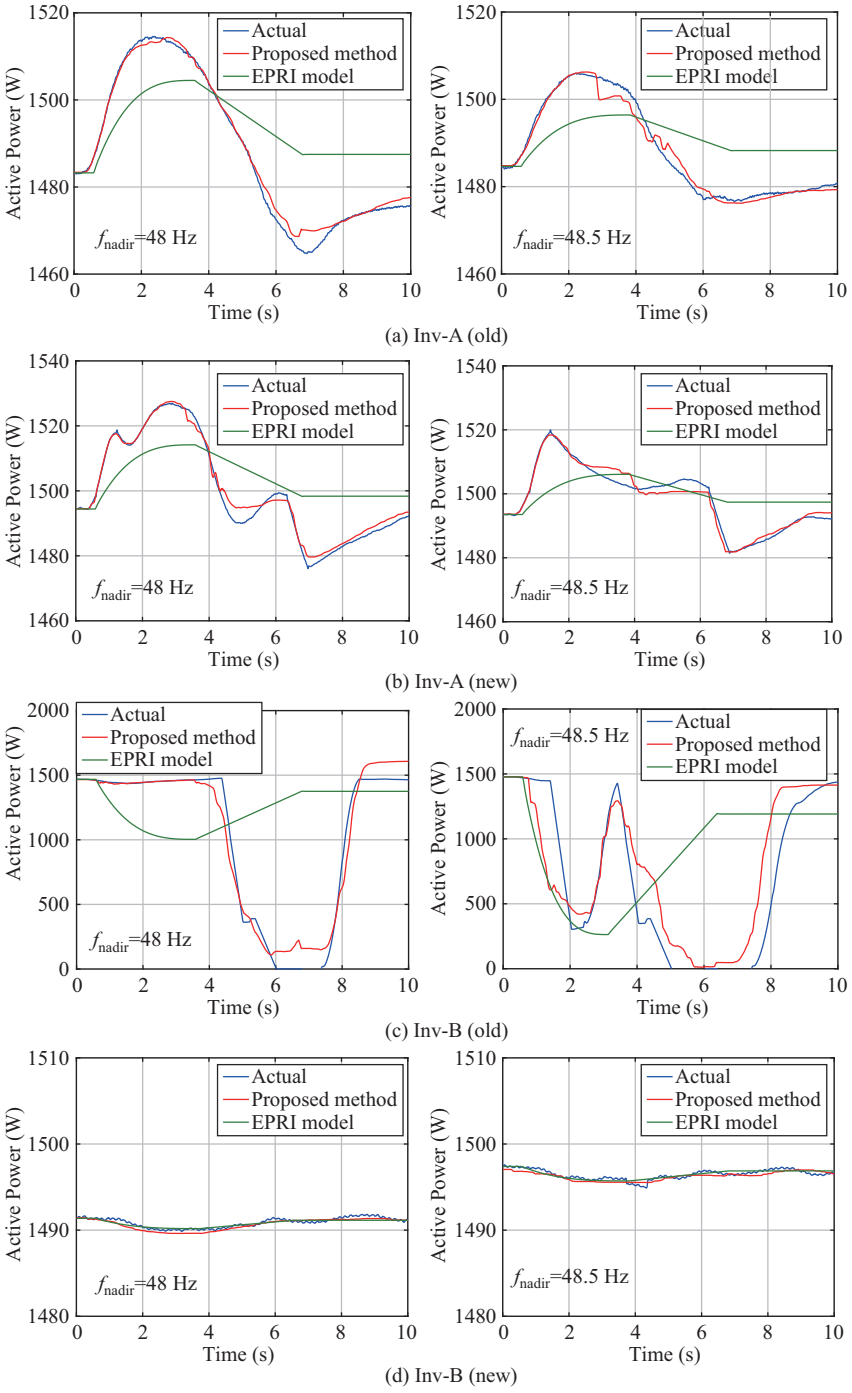

Fig. 11. Estimation verification of the developed dynamic frequency response model of different PV inverters with different frequency events.

and the lack of detailed inverter information. With the deployment of high precision sensors (e.g., PMUs) in distribution networks, data-driven approaches can provide new solutions for the power output estimation of complex electronic-based devices. This paper has completed the fundamental study for inverter frequency response estimation and an initial attempt to demonstrate the effectiveness of the machine-learning-based approaches for electronic-based energy resources. Although the proposed data-driven method uses neither frequency response of a large number of inverters nor the inverter control parameters for the estimation, its generalization capability is still assured as it is believed that the residential PV inverters with the same model and manufacturer would share the same control parameters which results in the same frequency response during the disturbance. Therefore, for PV inverters of the same manufacturer and model, a dedicated machine learning algorithm can be trained to estimate the corresponding frequency responses. The major challenges of the proposed approach lie in the construction of an informative and complete training database covering sufficient dynamic response of PV inverters of interest, which deserves further investigation with more inverters.

The developed inverter response estimation approach in this paper can provide a foundation for future feeder-level inverter frequency dynamic response estimation. These developed estimation models can be the components to form feeder level frequency dynamic responses. The network operators usually have the statistics (e.g., capacity, installed location, and manufacturer) of deployed PV inverters from the survey of customers. Therefore, it is achievable for network operators to obtain the composition of the inverters with different frequency response behaviors in the feeder. Then, the combined dynamic response of the PV inverters in the same feeder can be accurately predicted.

V. Conclusion

This paper has conducted fundamental research to extract new characteristics of frequency responses of small-scale PV inverters, which has the potential to influence the dynamics of the entire power grid. An inverter testing platform for small-scale PV inverters is established and then frequency response signatures of different inverters are extracted through extensive experiments. Finally, a data-driven approach is proposed and developed to estimate the active power response of small-scale PV inverters under different frequency disturbances.

The extracted signatures from the experimental results demonstrate that not all PV inverters are fully compliant with the frequency responses required by AS 4777. For example, two types of PV inverters are disconnected from the grid within the required connection range. Moreover, the frequency response behaviors are also different for the inverters from the same manufacturer or the inverters following the same standard. Some inverters (Inv-A) are grid-friendly by providing active power support during under-frequency events, while some inverters [Inv-B (old)] are very sensitive to frequency disturbances by rebooting the inverters frequently during the under-frequency events. The irregular frequency response behaviors are hard to describe by the traditional load model and they pose new challenges to the PV inverter response estimation. In response to these newly-emerging challenges, this paper has demonstrated that the machine learning-based approach could provide a good option for the frequency response estimation of PV inverters.

The presented study has demonstrated substantial benefits to network operators. The bottom-up study of the PV inverter response behaviors can help the network operators identify the root cause of the unexplainable dynamics during incidents for high solar PV integrated networks. Moreover, this paper can also help with top-down feeder-level and substation level load modelling as it reveals fundamental characteristics of electrical load components.

Acknowledgment

This study was performed in part or in full using equipment and infrastructure funded by the Australian Federal Government's Department of Education AGL Solar PV Education Investment Fund Research Infrastructure Project. The University of Queensland is the Lead Research Organization in partnership with AGL, First Solar and the University of New South Wales.

References

[1] R. F. Yan, N. A. Masood, T. K. Saha, F. F. Bai, and H. J. Gu, "The anatomy of the 2016 South Australia blackout: A catastrophic event in a high renewable network", *IEEE Transactions on Power Systems*, Vol. 33, no. 5, pp. 5374–5388, Sep. 2018.

[2] Y. J. Peng, Y. Li, K. Y. Lee, Y. Tan, Y. J. Cao, M. Wen, Y. W. Shen, M. M. Zhang, and W. G. Li, "Coordinated control strategy of PMSG and cascaded H-Bridge STATCOM in dispersed wind farm for suppressing unbalanced grid voltage", *IEEE Transactions on Sustainable Energy*, vol. 12, no. 1, pp. 349–359, Jan. 2021.

[3] H. J. Gu, R. F. Yan, T. K. Saha, "Review of system strength and inertia requirements for the national electricity market of Australia," *CSEE Journal of Power and Energy Systems*, vol. 5, no. 3, pp. 295–305, Sep. 2019.

[4] Australian PV Institute. [Online]. Available at http://pv-map.apvi.org.au /animation.

[5] Australian Energy Market Operator (AEMO), Response of existing PV inverters to frequency disturbances, AEMO report, April 2016.

[6] AEMO, Final report-Queensland and South Australia system separation on 25 August 2018, published on 10 January 2019.

[7] AEMO, Fault at Torrens Island Switchyard and Loss of Multiple Generating Units on 3 March 2017, published on 10 March 2017.

[8] *Grid Connection of Energy Systems via Inverters – Part 3: Grid Protection Requirements*, AS 4777.3-2005, 2005.

[9] *Grid Connection of Energy Systems via Inverters – Part 2: Inverter Requirements*, AS/NZS 4777.2:2015, 2015.

[10] WECC Dynamic Composite Load Model (CMPLDW) specifications. [Online]. http://home.engineering.iastate.edu/~jdm/ee554/WECC%20Composite%20Load%20Model%20Specifications%2001-27-2015.pdf

[11] B. Mather, O. Aworo, R. Bravo, and P. E. David Piper, "Laboratory testing of a utility-scale PV inverter's operational response to grid disturbances", in *2018 IEEE Power & Energy Society General Meeting*, Portland, OR, USA, 2018, pp. 1–5.

[12] R. J. Bravo, R. Yinger, S. Robles, and W. Tamae, "Solar PV inverter testing for model validation", in *2011 IEEE Power and Energy Society General Meeting*, Detroit, MI, USA, 2011, pp. 1–7.

[13] B. Mather and F. Ding, "Distribution-connected PV's response to voltage sags at transmission-scale," in *2016 IEEE 43rd Photovoltaic Specialists Conference*, Portland, OR, USA, 2016, pp. 2030–2035.

[14] Y. T. Tan, D. S. Kirschen, and N. Jenkins, "A model of PV generation suitable for stability analysis," *IEEE Transactions on Energy Conversion*, vol. 19, no. 4, pp. 748–755, Dec. 2004.

[15] D. Remon, A. M. Cantarellas, and P. Rodriguez, "Equivalent model of large-scale synchronous photovoltaic power plants," *IEEE Transactions on Industry Applications*, vol. 52, no. 6, pp. 5029–5040, Nov./Dec. 2016.

[16] J. T. Bi, W. Du, and H. F. Wang, "Aggregated dynamic model of grid-connected PV generation farms," in *International Conference on Renewable Power Generation*, Beijing, China, 2015.

[17] R. T. Guttromson, "Modeling distributed energy resource dynamics on the transmission system," *IEEE Transactions on Power Systems*, vol. 17, no. 4, pp. 1148–1153, Nov. 2002.

[18] S. N. Shao, M. Pipattanasomporn, and S. Rahman, "Development of physical-based demand response-enabled residential load models," *IEEE Transactions on Power Systems*, vol. 28, no. 2, pp. 607–614, May 2013.

[19] A. Grandjean, J. Adnot, and G. Binet, "A review and an analysis of the residential electric load curve models," *Renewable and Sustainable Energy Reviews*, vol. 16, no. 9, pp. 6539–6565, Dec. 2012.

[20] A. Bokhari, A. Alkan, R. Dogan, M. Diaz-Aguiló, F. De León, D. Czarkowski, Z. Zabar, L. Birenbaum, A. Noel, and R. E. Uosef, "Experimental determination of the ZIP coefficients for modern residential, commercial, and industrial loads," *IEEE Transactions on Power Delivery*, vol. 29, no. 3, pp. 1372–1381, Jun. 2014.

[21] X. Wang, Y. S. Wang, D. Shi, J. H. Wang, and Z. W. Wang, "Two-stage WECC composite load modeling: a double deep Q-learning networks approach", *IEEE Transactions on Smart Grid*, vol. 11, no. 5, pp. 4331–4344, Sep. 2020.

[22] M. Jin, H. Renmu, and D. J. Hill, "Load modeling by finding support vectors of load data from field measurements," *IEEE Transactions on Power Systems*, vol. 21, no. 2, pp. 726–735, May 2006.

[23] A. Ellis, M. R. Behnke, and R. T. Elliott, "Generic solar photovoltaic system dynamic simulation model specification", USDOE National Nuclear Security Administration (NNSA), United States, SAND2013–8876, 2013.

[24] P. Cicilio and E. Cotilla-Sanchez, "Evaluating measurement-based dynamic load modeling techniques and metrics," *IEEE Transactions on Power Systems*, vol. 35, no. 3, pp. 1805–1811, May 2020.

[25] I. F. Visconti, D. A. Lima, J. M. C. De Sousa Costa, and N. R. De B. C. Sobrinho, "Measurement-based load modeling using transfer functions for dynamic simulations," *IEEE Transactions on Power Systems*, vol. 29, no. 1, pp. 111–120, Jan. 2014.
[26] F. F. Bai, X. R. Wang, Y. L. Liu, X. Y. Liu, Y. Xiang, Y. Liu, "Measurement-based power system frequency dynamic response estimation using geometric template matching and recurrent artificial neural network," *CSEE Journal of Power and Energy Systems*, vol. 2, no. 3, pp. 10–18, Sep. 2016.
[27] E. O. Kontis, T. A. Papadopoulos, A. I. Chrysochos, and G. K. Papagiannis, "Measurement-based dynamic load modeling using the vector fitting technique," *IEEE Transactions on Power Systems*, vol. 33, no. 1, pp. 338–351, Jan. 2018.
[28] A. Arif, Z. Y. Wang, J. H. Wang, B. Mather, H. Bashualdo, and D. B. Zhao, "Load modeling-a review," *IEEE Transactions on Smart Grid*, vol. 9, no. 6, pp. 5986–5999, Nov. 2018.
[29] W. W. Price, K. A. Wirgau, A. Murdoch, J. V. Mitsche, E. Vaahedi, and M. El-Kady, "Load modeling for power flow and transient stability computer studies," *IEEE Transactions on Power Systems*, vol. 3, no. 1, pp.180–187, Feb. 1988.
[30] T. Hiyama, M. Tokieda, W. Hubbi, and H. Andou, "Artificial neural network based dynamic load modeling," *IEEE Transactions on Power Systems*, vol. 12, no. 4, pp. 1576–1583, Nov. 1997.
[31] Y. T. Ji, E. Buechler, and R. Rajagopal, "Data-Driven load modeling and forecasting of residential appliances", *IEEE Transactions on Smart Grid*, vol. 11, no. 3, pp. 2652–2661, May 2020.
[32] M. Segal and Y. Y. Xiao, "Multivariate random forests", *Wiley Interdisciplinary Reviews: Data Mining and Knowledge Discovery*, vol. 1, no. 1, pp. 80–87, Jan./Feb. 2011.

Feifei Bai (S'13–M'16–SM'21) received B.S. and Ph.D. degrees in Power Systems and its Automation from Southwest Jiaotong University, China, in 2010 and 2016, respectively. She was a joint-Ph.D. student at the University of Tennessee, Knoxville, TN, USA, from 2012 to 2014. She is currently a senior lecturer in the School of Engineering and Built Environment at Griffith University and an Advance Queensland Fellow in the School of Information Technology and Electrical Engineering, University of Queensland, Australia. Her research interests include renewable energy integration and big data technology applications in power grids.

Yi Cui (M'19–SM'21) received B.Eng. and M.Eng. degrees from Southwest Jiaotong University, Chengdu, China, in 2009 and 2012, respectively, and received a Ph.D. degree in Electrical Engineering at the University of Queensland, Brisbane, Australia, in 2016. Dr. Cui has been a Research Fellow in the Department of Electrical Engineering and Computer Science, University of Tennessee, Knoxville, TN, USA since May 2016. Currently, he is a Research Fellow in the School of Information Technology and Electrical Engineering, the University of Queensland, Australia. His research interests include wide-area monitoring and control, data analytics and machine learning of distribution networks, condition assessment and fault diagnosis of power transformers.

Ruifeng Yan (S'09–M'12) received a B.Eng. degree in Automation from the University of Science and Technology, China, in 2004, an M.Eng. degree in Electrical Engineering from the Australian National University, Australia, in 2007, and a Ph.D. degree in Power and Energy Systems from the University of Queensland, Australia, in 2012. He is currently a senior lecturer at the School of Information Technology and Electrical Engineering, University of Queensland, Australia. His research interests include power system operations and analysis and renewable energy integration into power networks.

Tapan Kumar Saha (M'93–SM'97–F'19) received a B.Sc. Engineering (electrical and electronic) in 1982 from the Bangladesh University of Engineering & Technology, Bangladesh, an M.Tech. degree in 1985 from the Indian Institute of Technology, India and a Ph.D. degree in 1994 from the University of Queensland, Australia. Tapan is currently a professor in the School of Information Technology and Electrical Engineering, University of Queensland, Australia. His research interests include condition monitoring of electrical plants, power systems and power quality.

Huajie Gu (S'16) received a B.Eng. degree in Automation from Nanjing Technical University, Nanjing, China, in 2011, an M.Eng. degree in Control Theory and Control Engineering from Tongji University, Shanghai, China, in 2014, and a Ph.D. degree in Electrical Engineering from The University of Queensland, Brisbane, Australia, in 2019. He is currently working as a Dispatch Engineer with the Australian Energy Market Operator, Brisbane, Australia. His research interests include electricity market and power system stability and control.

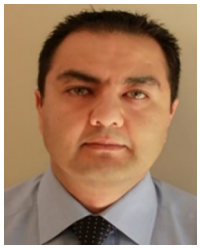

Daniel Eghbal (S'05–M'10) received a B.S. degree in Electrical Engineering from Ferdowsi University of Mashhad, Iran, in 1998, an M.S. degree in Power System Engineering from Tarbiat Modares University, Iran, in 2001, and a Ph.D. degree from Hiroshima University, Japan, in 2009. He is a Manager for the Future Network Strategy with Energy Queensland, Australia. His research interests include DER integration, and decentralization of distribution networks.